Light-Emitting Color Barcode Nanowires Using Polymers: Nanoscale Optical Characteristics

Dong Hyuk Park,[†,§] Young Ki Hong,[†] Eun Hei Cho,[†] Mi Suk Kim,[†] Dae-Chul Kim,[‡] Jihee Bang,[‡] Jeongyong Kim,[‡,⊥,*] and Jinsoo Joo[†,⊥,*]

[†]Department of Physics, Korea University, Seoul 136-713, Korea, [‡]Department of Physics, University of Incheon, Incheon 406-772, Korea, and [§]Department of Chemical and Biological Engineering, Korea University, Seoul 136-713, Korea. [⊥]These authors contributed equally to this work.

ABSTRACT We report on the light-emitting color barcode nanowires (LECB-NWs), which were fabricated by alternating the electrochemical polymerization of light-emitting polymers with various luminescence colors and efficiencies. The nanoscale photoluminescence characteristics of LECB-NWs were investigated using a laser confocal microscope with a high spatial resolution. The alternating light emissions of the LECB-NWs showed orange-yellow, red, and green colors due to the serial combination of poly(3-butylthiophene), poly(3-methylthiophene), and poly(3,4-ethylenedioxythiophene), respectively, with distinct luminescence intensities. The optical detection sensitivity and stability of LECB-NWs have been enhanced through a nanoscale Cu metal coating onto the NWs, based on surface plasmon resonance coupling and protection against oxidation. The flexibility of the LECB-NWs has been investigated through the folding and unfolding of the NWs by an applied nanotip impetus. The flexible LECB-NWs can be used as highly sensitive optical identification nanosystems for nanoscale or microscale products with complex physical shapes.

KEYWORDS: barcode · nanowire · light-emitting polymer · hybrid nanomaterial · nanoscale optical characteristics

With the development of nanotechnology (NT) and biotechnology (BT), products and devices related to NT and BT have become smaller (on a scale of micrometers or nanometers) and more complex, and they must have identification codes for applications and commercial uses.[1−3] Conventional black and white barcodes have been used for the identification of commercial products through optical reflection. Recently, inorganic metal-based or magnet-based barcode nanowires (NWs) have been studied for the identification of nanosized products, nanoscale magnetic memory, biological sensing, nanoswitches, and transistors.[4−10] For the effective identification of nanosized products with complex physical shapes, the identifying sensitivity, accuracy, flexibility, and stability of optical barcode nanomaterial should be improved in combination with proper detecting tools. One such promising optical barcode nanomaterial consists of flexible light-emitting color barcode nanowires (LECB-NWs) with intrinsically light-emitting polymers, which can also be adapted to biological sensing.[11−15]

Hybrid nanostructures of light-emitting polymers with inorganic metals such as Au, Ag, and Ni have been applied to luminescence enhancement and DNA sensing through surface plasmon (SP) resonance coupling.[16−18] When the SP energy of nanoscale metals is closely matched with the photon energy of light-emitting polymers, the resulting resonance can lead to an energy transfer between the nanoscale materials, resulting in enhanced photoluminescence (PL) efficiency.[19] The nanoscale metal coating on the LECB-NWs can contribute to the increase of the identifying sensitivity and stability as a nanoscale barcode, through the SP resonance coupling and protection against oxidation.

We report on the fabrication and nanoscale optical and structural characteristics of LECB-NWs consisting of various light-emitting polymers: poly(3-butylthiophene) (P3BT), poly(3-methylthiophene) (P3MT), and poly(3,4-ethylenedioxythiophene) (PEDOT). The code compartments of P3BT, P3MT, and PEDOT NWs of the LECB-NWs emitted orange-yellow, red, and green colors, respectively. Distinct PL intensities at the nanoscale were detectable using a laser confocal microscope (LCM) and color charge-coupled device (CCD) images. The PL efficiency and stability of an isolated single strand of the P3BT-PEDOT LECB-NWs increased considerably by nanoscale Cu metal coating *via* an energy transfer effect in a surface plasmon resonance (SPR) coupling.[16,17] The bending capability and flexibility of the LECB-NWs were also confirmed. Three different luminescence colors emitted from the P3BT-P3MT-PEDOT/Cu

*Address correspondence to jeongyong@incheon.ac.kr, jjoo@korea.ac.kr.

Received for review May 19, 2010 and accepted August 05, 2010.

Published online August 13, 2010. 10.1021/nn101096m

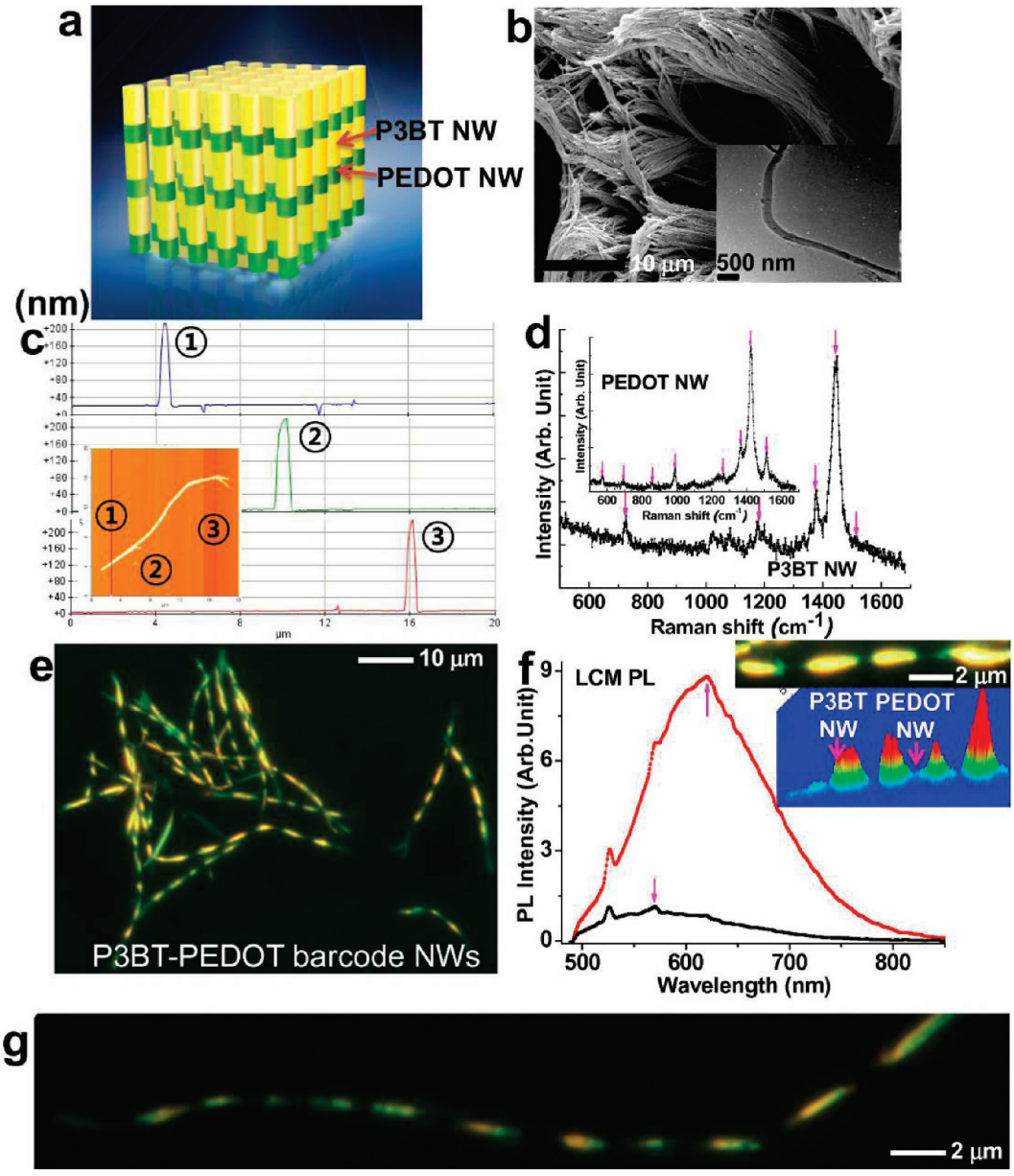

Figure 1. (a) Schematic illustration of polymer-based LECB-NW array. (b) SEM image of bundle of flexible P3BT-PEDOT LECB-NWs. Inset: magnified TEM image of a single strand of the LECB-NWs. (c) Topological analysis of the diameter of the LECB-NW through scanning AFM. Inset: AFM topography image of LECB-NW. (d) LCM Raman spectrum of P3BT NW compartments in the P3BT-PEDOT LECB-NW. Inset: LCM Raman spectrum of PEDOT NW compartments in the same LECB-NW. (e) Color CCD image of dispersed P3BT-PEDOT LECB-NWs at fixed excitation wavelength (λ_{ex} = 435 nm). (f) Comparison of LCM PL spectra of the P3BT and PEDOT compartments of the single LECB-NW. Insets: Color CCD and three-dimensional LCM PL images of the single LECB-NW. (g) Luminescence color CCD image of the single P3BT-PEDOT LECB-NW with 22 compartments.

LECB-NWs were selectively distinguished in the mixture states with other LECB-NWs.

RESULTS AND DISCUSSION

Light-Emitting Color Barcode NWs Using P3BT and PEDOT. Figure 1a shows a schematic illustration of the LECB-NWs consisting of two different light-emitting polymer NWs. We observed a homogeneous array of the flexible polymer NWs from SEM image (Figure 1b). A NW diameter of ~210 ± 20 nm was observed from AFM image and its topology analysis (Figure 1c), which is in agreement with the TEM image (inset of Figure 1b). We found an alternating of P3BT and PEDOT materials based on our analysis of LCM Raman spectra for the single NW (Figure 1d).[20,21] The Raman characteristic peaks at 726 and 1449 cm^{-1} correspond to symmetric C−S−C ring deformation and symmetric C_α=C_β stretching vibration of P3BT material (Figure 1d), and those at 574 and 990 cm^{-1} correspond to oxyethylene ring deformation of PEDOT (inset of Figure 1d). These were alternately observed through the scan of a focused laser and detector along a single NW in the LCM Raman experiments (Figure 1d and see Supporting Information for a more detailed analysis). The alternating light emissions of the

TABLE 1. Synthetic Conditions of P3BT, P3MT, and PEDOT Compartment of the LECB-NWs

	synthetic condition					
	P3BT		PEDOT		P3MT	
length of compartments (μm)	applied current density (mA/cm^2)	polymerization time (s)	applied current density (mA/cm^2)	polymerization time (s)	applied current density (mA/cm^2)	polymerization time (s)
1	0.6	60	0.2	60		
2	0.6	90	0.4	90	1.7	60
4	0.6	120	0.4	120		
6	0.6	150				

bright orange-yellow and green colors due to the distinct light emission characteristics of the P3BT and PEDOT materials, respectively, were clearly observed in a color CCD image of the P3BT-PEDOT LECB-NWs, as shown in Figure 1e. The code length of the P3BT and PEDOT NW compartments was estimated to be 2−4 and 1−4 μm, respectively.

Nanoscale luminescence characteristics of a single strand of P3BT-PEDOT LECB-NWs were investigated through LCM and color CCD experiments. Figure 1f shows the LCM PL spectra of P3BT and PEDOT compartments obtained from the same single LECB-NW. The LCM PL peak for the P3BT and PEDOT compartments in the same single NW was detected at ~626 nm (*i.e.*, orange-yellow light emission) and ~554 nm (*i.e.*, green light emission), respectively. The LCM PL peak intensity and integrated area of the compartments of the P3BT NW were approximately 9 times higher than those of the PEDOT NW. These observations were confirmed by the color CCD image of the single LECB-NW (inset of Figure 1f). The differences in the PL intensities of the P3BT and PEDOT compartments in the NWs were due to the energy band gap and chemical structure rather than a difference in the length of the compartments.[20,24] We also controlled the length and the number of repeated units of the polymer NW code compartments through polymerization conditions in the electrolyte. For example, a single strand of other P3BT-PEDOT LECB-NWs having a total of 22 compartments has been fabricated (Figure 1g). To fabricate the 22 compartments of the LECB-NWs, the number of dipping was 11 times per one electrolyte, and the alternating dipping was performed. The lengths of the P3BT and PEDOT NW compartments were controlled to be 1−2 μm, which were electrochemically polymerized during of 60−90 s with applied current density (0.6 mA/cm^2 for P3BT and 0.2−0.4 mA/cm^2 for PEDOT), respectively. The other LECB-NWs with different lengths and repeated units are also shown in Figure S3 (Supporting Information). Detailed synthetic conditions of the different P3BT-PEDOT LECB-NWs are listed in Table 1. We suggest that the discrete luminescences due to the P3BT and PEDOT compartments in the LECB-NWs can introduce various encoding and decoding patterns.

Nanoscale Cu Metal-Coated Light-Emitting Color Barcode NWs. Enhanced luminescence efficiency of the polymer-based light-emitting NWs can be expected *via* a nanoscale metal coating through an energy transfer effect in a SPR coupling.[23,24] Figure 2a shows a schematic illustration of the nanoscale Cu metal-coated P3BT-PEDOT (P3BT-PEDOT/Cu) LECB-NW. The formation of Cu metal-coated P3BT-PEDOT LECB-NWs was confirmed through HR-TEM experiments (Figure 2b). From the magnified HR-TEM image, the total diameter of the single P3BT-PEDOT/Cu LECB-NW and the thickness of the outside Cu were ~200 and ~10 nm, respectively. We observed the fine and periodic patterns of the outer tube representing the crystalline structure of the Cu material (inset of Figure 2b). Figure 2c,d compares the three-dimensional (3-D) LCM PL images for an isolated single strand of the P3BT-PEDOT and P3BT-PEDOT/Cu LECB-NWs, respectively, in the same LCM experimental conditions. The measured voltages of the LCM PL intensities of the hybrid parts of the P3BT/Cu and PEDOT/Cu compartments were 1.8−2.0 V and 26−30 mV, respectively, while those of the P3BT and PEDOT compartments without the Cu coating were 140−180 mV and 22−25 mV, respectively (Figure 2c,d). The measured voltages of the LCM PL intensities for the hybrid P3BT/Cu compartments were approximately 10−14 times higher than those of the P3BT compartments. The LCM PL peak (at $\lambda \cong 635$ nm) intensity and integrated area of the compartments of the P3BT/Cu NW were approximately 80 times higher than that (at $\lambda \cong 544$ nm) of the PEDOT/Cu NW (Figure 2e and its inset). The SP energy (~2.1 eV or 585 nm) of the nanoscale Cu was closely matched with the emissive photon energy of the P3BT materials, and SPR coupling occurred that induced an energy transfer between the nanoscale Cu and P3BT materials.[24] This induced the considerable enhancement of the PL efficiency for the hybrid P3BT/Cu compartments. The results indicate that the optically identifying sensitivity of the P3BT-PEDOT LECB-NWs was considerably enhanced through the nanoscale Cu coating. It is noted that the main LCM PL peaks of P3BT and PEDOT compartments in various LECB-NWs were detected at 620−635 and 544−554 nm, respectively. The deviation of the position of the main LCM PL peaks and their broadness might originate from the near-

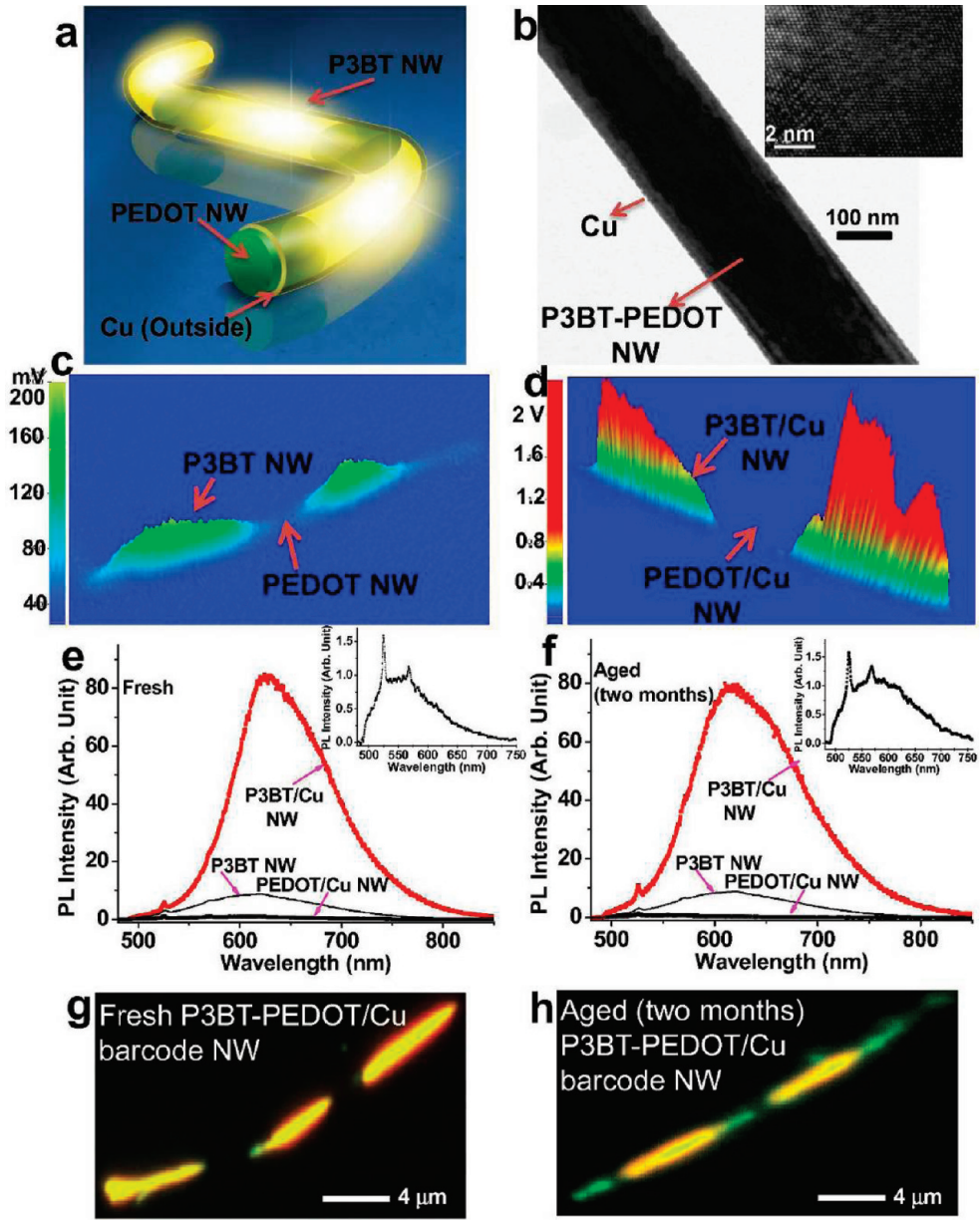

Figure 2. (a) Schematic illustration of P3BT-PEDOT/Cu LECB-NW. (b) HR-TEM image of the single P3BT-PEDOT/Cu LECB-NW. Inset: Magnified HR-TEM image of the outside Cu part of the LECB-NW. (c) Three-dimensional LCM PL image of a single strand of fresh P3BT-PEDOT LECB-NW without Cu metal. (d) Three-dimensional LCM PL image of the fresh P3BT-PEDOT/Cu single LECB-NW. Comparison of LCM PL spectra of (e) the fresh P3BT/Cu and PEDOT/Cu compartments and of (f) the aged (2 months) P3BT/Cu and PEDOT/Cu compartments. Insets: LCM PL spectra of the fresh and aged PEDOT/Cu compartments for a reference. (g,h) Luminescence color CCD images of an isolated single strand of the fresh and aged (2 months) P3BT-PEDOT/Cu LECB-NWs, respectively.

field characteristics of PL spectra of the light-emitting polymer nanomaterials.

To study the environmental stability of the identifying and detecting capability, we compared the LCM PL images, spectra, and color CCD images for the fresh and aged P3BT-PEDOT/Cu LECB-NWs. The voltages of the LCM PL intensities of the hybrid P3BT/Cu and PEDOT/Cu compartments of a single strand of aged P3BT-PEDOT/Cu LECB-NW after 2 months of exposure to the atmosphere were 1.6−1.8 V and 23−27 mV, respectively. These LCM PL voltage values slightly decreased but were comparable with those of the fresh P3BT-PEDOT/Cu LECB-NWs because of the oxidation protection from the nanoscale Cu coating. These results were confirmed by measurements of the LCM PL spectra (Figure 2f), in which LCM PL peak positions and intensities of the aged samples were comparable with those of the fresh samples. Figure 2g,h shows color CCD images of the fresh and aged single P3BT-PEDOT/Cu LECB-NW, respectively. The green color light emission of PEDOT/Cu compartments in the aged LECB-NWs was observed, while the orange-yellow color light emission from the P3BT/Cu compartments was more dominant for the fresh LECB-NWs (Figure 2g,h). The difference of the CCD

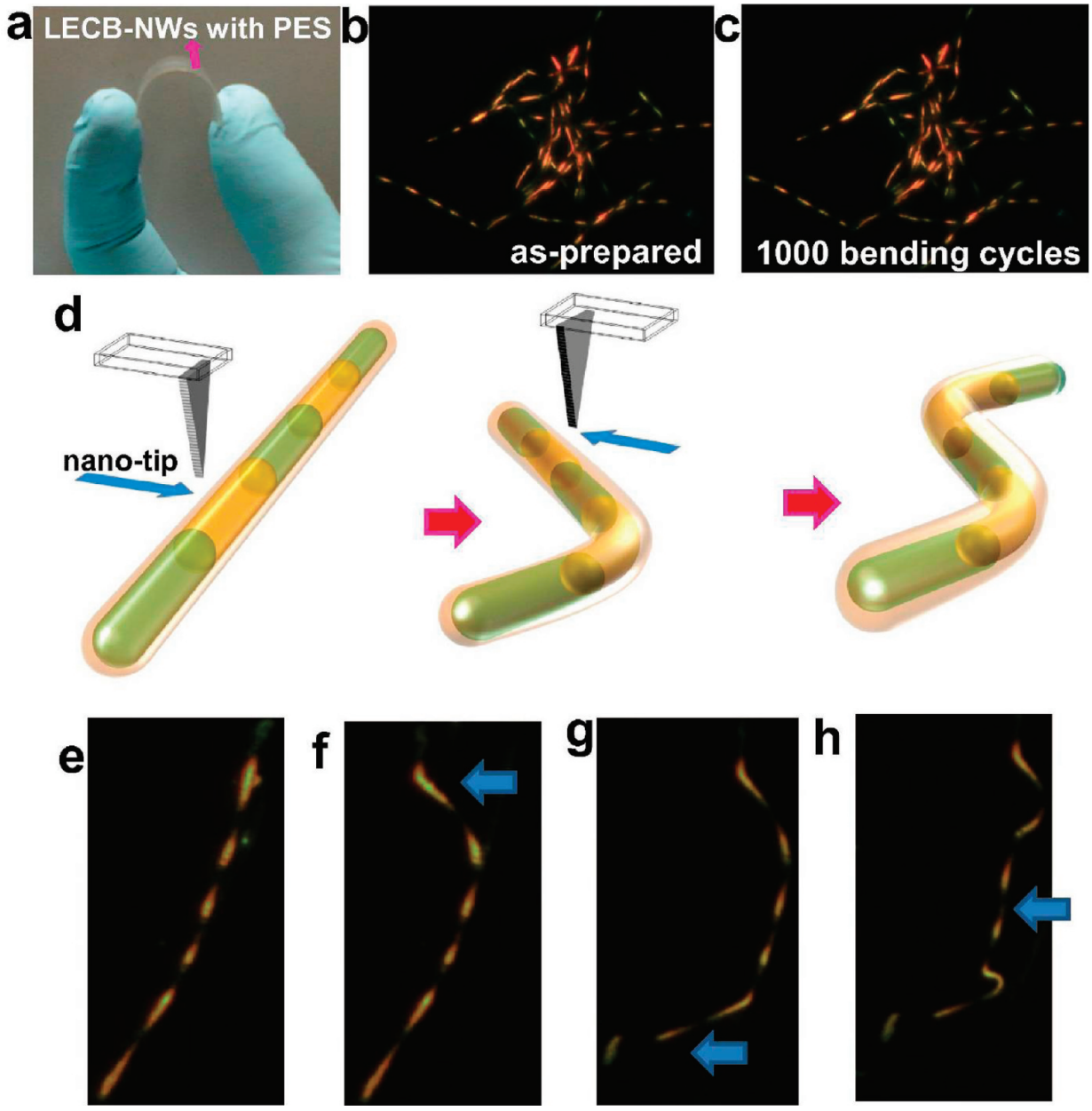

Figure 3. (a) Camera image of flexible P3BT-PEDOT/Cu LECB-NWs fixed on the PES substrate. (b) Luminescence color CCD image of as-prepared P3BT-PEDOT/Cu LECB-NWs on the PES substrate. (c) Luminescence color CCD image of P3BT-PEDOT/Cu LECB-NWs on the PES substrate after bending (1000 cycles). (d) Schematic illustrations of flexibility experiments for the LECB-NWs applying nanotip impetus. (e−h) Luminescence color CCD images of the P3BT-PEDOT/Cu LECB-NW after the applied impetus. The arrows represent the positions of the applied impetus by nanotip.

images in Figure 2g,h could be due to the distinct contrast ratio between the brighter parts of the P3BT/Cu and the relatively dark parts of the PEDOT/Cu compartments for the fresh samples. We consistently observed distinct luminescence characteristics, that is, alternating light emissions of orange-yellow and green colors for the bundle of 1 year aged P3BT-PEDOT/Cu NWs (see Supporting Information Figure S6). These results imply that the Cu metal-coated P3BT-PEDOT LECB-NWs can function as promising optical barcode NWs in terms of highly sensitive light emission with long-term stability for identification.

Flexibility of Light-Emitting Color Barcode NWs. We performed bending and flexibility experiments on the P3BT-PEDOT/Cu LECB-NWs. Figure 3a shows a photograph of the bending of the NWs fixed onto the polyethersulfone (PES) flexible substrate. The alternating light emissions of the orange-yellow and green colors of the P3BT-PEDOT/Cu LECB-NWs on the PES substrate were clearly observed in the color CCD image (Figure 3b). We consistently observed distinct luminescence characteristics after bending, for example, alternating light emissions of orange-yellow and green colors after a thousand bending cycles of the P3BT-PEDOT/Cu NWs

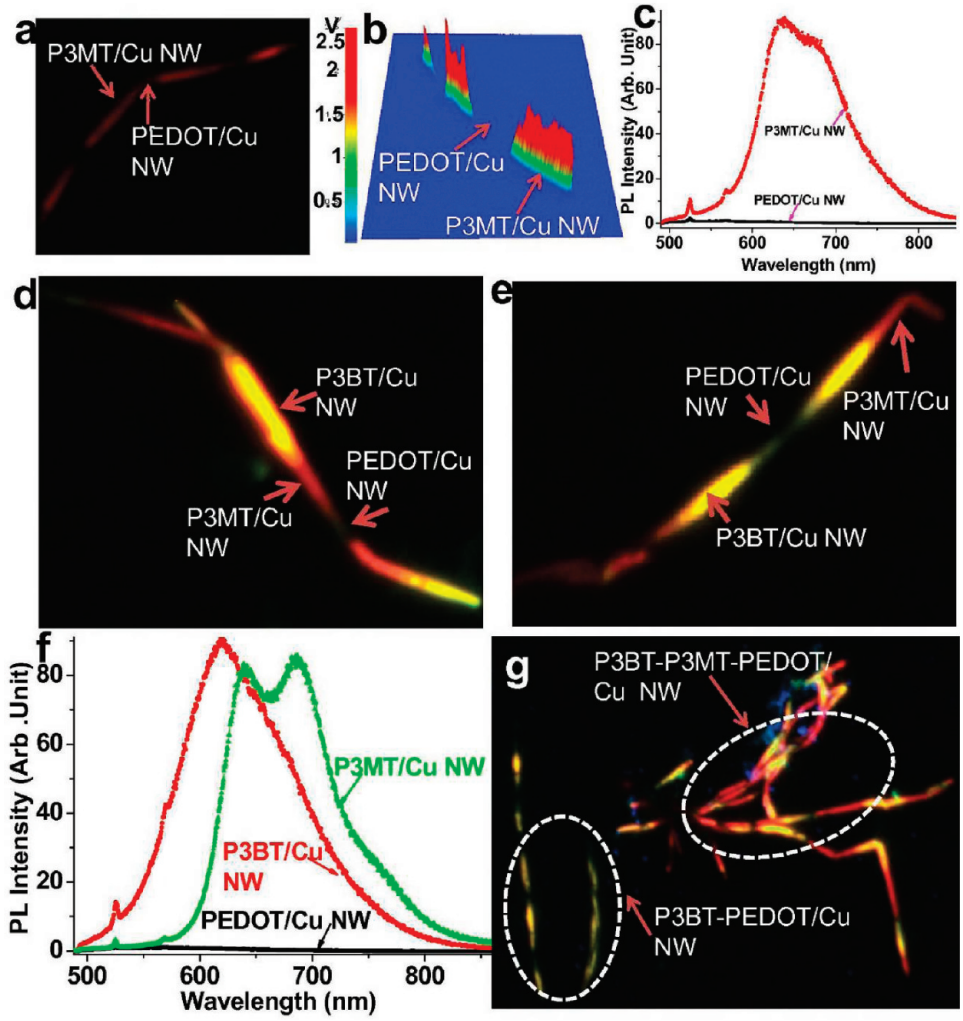

Figure 4. (a) Color CCD image of the P3MT-PEDOT/Cu single LECB-NW. (b) Three-dimensional LCM PL image of the P3MT-PEDOT/Cu single LECB-NW. (c,d) Color CCD images of the P3BT-P3MT-PEDOT/Cu single LECB-NW and the P3MT-P3BT-PEDOT/Cu single LECB-NW, respectively. (e) LCM PL spectra of P3MT/Cu, P3BT/Cu, and PEDOT/Cu compartments in P3BT-P3MT-PEDOT/Cu single LECB-NW. (f) Color CCD image of the mixture of the P3MT-PEDOT/Cu and P3BT-P3MT-PEDOT/Cu LECB-NWs.

(Figure 3c). The flexibility of these NWs was investigated through an applied impetus to some parts of the NW using a nanotip. Depending on the position of the nanotip impetus (Figure 3d), we observed the folding and unfolding of the LECB-NW, implying the flexibility of the NW (Figure 3e−h) (see Supporting Information movie). These results imply that the P3BT-PEDOT/Cu LECB-NWs fabricated in the study can be promising optical barcode NWs with durability and flexibility. The macroscopic optical detection for the P3BT-PEDOT/Cu LECB-NWs was also performed by using a conventional digital camera under light exposure. We observed the black spots for the aggregated LECB-NWs in the magnified digital camera images (Figure S8b). However, we could not observe the distinct luminescence color and intensity of the aggregated LECB-NWs with the naked eye (Figure S8, Supporting Information).

Decoding Study Using a Mixture of Various Barcode NWs. To study decoding ability using a mixture of various LECB-NWs, we fabricated different LECB-NWs consisting of P3MT and PEDOT materials coated with Cu (P3MT-PEDOT/Cu). Figure 4a shows the distinct luminescent colors of red and green for the P3MT/Cu and PEDOT/Cu compartments in the same LECB-NW, respectively. Figure 4b shows a 3-D LCM PL image for the P3MT-PEDOT/Cu single LECB-NW. The measured voltages of the LCM PL intensities of the P3MT/Cu and PEDOT/Cu compartments were 2.2−2.5 V and 28−32 mV, respectively (Figure 4b). We also fabricated LECB-NWs consisting of three different light-emitting polymers (P3MT, P3BT, and PEDOT NWs) coated with nanoscale Cu. We confirmed the formation of P3MT-P3BT-PEDOT/Cu LECB-NWs from the LCM Raman spectra (see Supporting Information Figure S9 and Tables S1−S3). The red, orange-yellow, and green luminescence colors corresponding to the P3MT/Cu, P3BT/Cu, and PEDOT/Cu compartments in the same LECB-NW, respectively, were observed from the color CCD images (Figure 4d,e). Through the change of synthetic ordering of the polymers in the LECB-NWs, we obtained various LECB-NWs

with different luminescent patterns (Figure 4d,e). Figure 4f compares LCM PL spectra for P3MT/Cu, P3BT/Cu, and PEDOT/Cu code compartments in the same LECB-NW. The LCM PL peaks for the P3MT/Cu, P3BT/Cu, and PEDOT/Cu compartments were detected at 640−685 nm (*i.e.*, red light emission), 620 nm (*i.e.*, orange-yellow light emission), and ~545 nm (*i.e.*, green light emission), respectively. The LCM PL peak intensity and integrated area of the compartments of the P3MT/Cu NW and the P3BT/Cu NW were approximately 85 and 90 times higher than those of the PEDOT/Cu NW, respectively. From the color CCD image for the mixture of two different LECB-NWs, the three luminescence colors (red, orange-yellow, and green) due to the P3BT-P3MT-PEDOT/Cu LECB-NWs were selectively distinguished from the two luminescence colors due to P3BT-PEDOT/Cu LECB-NWs, as shown in Figure 4g, because of the distinct luminescence characteristics in the mixture states.

CONCLUSION

Light-emitting color barcode nanowires combined with different luminescent polymers were fabricated by alternating the electrochemical synthetic method. With various combinations of distinguishable PL intensities and colors in each compartment using different light-emitting polymers, encoding and decoding in the LECB-NWs are possible. Because the length and the number of repeated unit of the code, compartments of the LECB-NWs were controlled through the synthetic conditions, a variety of encoding can be guaranteed. Upon single wavelength excitation, the LECB-NWs can be readily detectable for identification by means of a microscope and/or spectrometer systems, which provides accuracy, sensitivity, security, and convenience in the decoding process. Optically detecting sensitivity and stability of the polymer-based LECB-NWs have been enhanced through nanoscale Cu coatings to the NWs based on SPR coupling and protection against oxidation. The LECB-NWs have flexibility, bending capability, and compatibility with biomaterials because of the polymer-based systems. Therefore, they can be applied to the identification of nanoscale or microscale products with complex physical shapes.[25−27]

EXPERIMENTAL SECTION

Fabrication of Light-Emitting Color Barcodes NWs. The LECB-NWs were fabricated by alternating the electrochemical polymerization of P3BT, P3MT, and PEDOT materials based upon an anodic alumina oxide (Al_2O_3) nanoporous template.[20,22,28] Three electrolyte batches for the synthesis of P3BT, P3MT, and PEDOT materials were prepared. We used an ionic liquid, 1-butyl-3-methylimidazolium hexafluorophosphate ($BMIMPF_6$) for the electrochemical polymerization of 3-butylthiophene (3BT), 3-methylthiophene (3MT), and 3,4-ethylenedioxythiophene (EDOT) monomers. It is noted that the use of the $BMIMPF_6$ ionic liquid contributed to improve the light emission property for the polymers.[29] Acetonitrile (CH_3CN) was used as a solvent. The 3BT (96% purified), 3MT (98% purified), EDOT (99% purified) monomers, and $BMIMPF_6$ (96% purified) were purchased from Sigma-Aldrich Co. and used without further purification. To form alternating P3BT, P3MT, and PEDOT NWs, we performed an alternative dipping process in two or three electrolyte batches including 3BT, 3MT, and EDOT monomers. The length and repeated unit of the P3BT, P3MT, and PEDOT NW code compartments were controlled through variation of the applied current density (0.6, 1.7, or 0.2−0.4 mA/cm^2), polymerization time (60−120 s), and the number of dipping times.[20,22,28] Detailed synthetic conditions of each compartment are listed in Table 1. After the formation of the LECB-NWs, a hydrofluoric (HF) acid solvent was used to remove only the Al_2O_3 template, resulting in the formation of LECB-NWs (Figure 1 and Figure S1 in Supporting Information). To fabricate the hybrid Cu-coated LECB-NWs, Cu metal was directly potentiostatically coated onto the surface of the LECB-NWs including the Al_2O_3 template.[23,24] For the coating Cu metal, the electrolytes consisted of $CuSO_4 \cdot 5H_2O$ (238 g/L) with sulfuric acid (21 g/L) in distilled water. We used cyclic voltammetry (Bioanalytical Systems Inc., EC Epsilon) for the electrochemical synthesis. For the nanoscale coating Cu metal, the applied bias was potentiostatically at 0 V (*vs* Ag/AgCl) for 10 min. A similar fabrication method for the nanoscale metal coating was reported previously.[30] The LECB-NWs were homogeneously dispersed in methanol solution after removal of the Al_2O_3 nanoporous template and then ultrasonicated for 3 s with a power of 70 W (BRANSON Co. Ultrasonic Cleaner). When the power of the sonication became stronger and operation time increased, the LECB-NWs were broken. It should be noted that the nanoscale metal coating improved the mechanical stability of the connections in the LECB-NWs because of the protection of the junctions between polymer compartments by metal coating. For the LCM experiments, the dispersed solution of the LECB-NWs was drop-cast onto a slide glass and then dried in a vacuum oven (below 10^{-3} Torr) for 30 min at room temperature.

Measurements for Nanoscale Optical and Structural Characteristics. The formation of the LECB-NWs and their hybrid nanosystems with Cu metal was visualized by using AFM (PSIA, XE-120), SEM (JEOL, JSM-5200), TEM (JEOL, JEM-2010), and HR-TEM (JEOL, JEM-3010) images. The luminescence color CCD images of the NWs were measured using an AVT Marlin F-033C (λ_{ex} = 435 nm). To compare the brightness of CCD images under the same experimental conditions, the exposure time of the light was fixed at 1 s. We measured the solid-state PL images, spectra, and Raman spectra for an isolated single strand of the LECB-NWs using a LCM built around an inverted optical microscope (Axiovert 200, Zeiss GmbH). The 488 nm line of an unpolarized argon ion laser was used for the LCM PL excitation, and the 633 nm line of a He−Ne gas laser was used for Raman excitation. The spot size of the focused laser beam on the sample was estimated to be about 190 nm. The laser power incident on the sample and the acquisition time for each PL spectrum were fixed in the LCM PL measurements at 1 μW and 1 s, respectively. Detailed methods for the LCM PL and Raman experiments were reported previously.[31,32]

Acknowledgment. This work was supported by a National Research Foundation (NRF) of Korea grant funded by the Korea government (MEST; R0A-2007-000-20053-0).

Supporting Information Available: Description of detail analysis of LCM Raman spectra of LECB-NWs, and sensitivity and stability study of nanoscale Cu-coated LECB-NWs. This material is available free of charge *via* the Internet at http://pubs.acs.org.

REFERENCES AND NOTES

1. Gudiksen, M. S.; Lauhon, L. J.; Wang, J.; Smith, D. C.; Lieber, C. M. Growth of Nanowire Superlattice Structures for Nanoscale Photonics and Electronics. *Nature* **2002**, *415*, 617–620.
2. Love, J. C.; Urbach, A. R.; Prentiss, M. G.; Whitesides, G. M.

Three-Dimensional Self-Assembly of Metallic Rods with Submicron Diameters Using Magnetic Interactions. *J. Am. Chem. Soc.* **2003**, *125*, 12696–12697.
3. Subramanian, V.; Frechet, J. M. J.; Chang, P. C.; Huang, D. C.; Lee, J. B.; Molesa, S. E.; Murphy, A. R.; Redinger, D. R.; Volkman, S. K. Progress toward Development of All-Printed RFID Tags: Materials, Processes, and Devices. *Proc. IEEE* **2005**, *93*, 1330–1338.
4. Nicewarner-Peña, S. R.; Freeman, R. G.; Reiss, B. D.; He, L.; Peña, D. J.; Walton, I. D.; Cromer, R.; Keating, C. D.; Natan, M. J. Submicrometer Metallic Barcodes. *Science* **2001**, *294*, 137–141.
5. Urbach, A. R.; Love, J. C.; Prentiss, M. G.; Whitesides, G. M. Sub-100 nm Confinement of Magnetic Nanoparticles Using Localized Magnetic Field Gradients. *J. Am. Chem. Soc.* **2003**, *125*, 12704–12705.
6. Pregibon, D. C.; Toner, M.; Doyle, P. S. Multifunctional Encoded Particles for High-Throughput Biomolecule Analysis. *Science* **2007**, *315*, 1393–1396.
7. Park, S.; Chung, S.-W.; Mirkin, C. A. Hybrid Organic−Inorganic, Rod-Shaped Nanoresistors and Diodes. *J. Am. Chem. Soc.* **2004**, *126*, 11772–11773.
8. Chung, H.-J.; Jung, H. H.; Cho, Y.-S.; Lee, S.; Ha, J.-H.; Choi, J. H.; Kuk, Y. Cobalt−Polypyrrole−Cobalt Nanowire Field-Effect Transistors. *Appl. Phys. Lett.* **2005**, *86*, 213113-1–213113-3.
9. Lee, J. H.; Wu, J. H.; Liu, H. L.; Cho, J. U.; Cho, M. K.; An, B. H.; Min, J. H.; Noh, S. J.; Kim, Y. K. Iron−Gold Barcode Nanowires. *Angew. Chem., Int. Ed.* **2007**, *46*, 3663–3667.
10. Qin, L.; Banholzer, M. J.; Millstone, J. E.; Mirkin, C. A. Nanodisk Codes. *Nano Lett.* **2007**, *7*, 3489–3493.
11. Wilson, R.; Cossins, A. R.; Spiller, D. G. Encoded Microcarriers for High-Throughput Multiplexed Detection. *Angew. Chem., Int. Ed.* **2005**, *45*, 6104–6117.
12. Allen, C. N.; Lequeux, N.; Chassenieux, C.; Tessier, G.; Dubertret, B. Optical Analysis of Beads Encoded with Quantum Dots Coated with a Cationic Polymer. *Adv. Mater.* **2007**, *19*, 4420–4425.
13. Chen, L.; McBranch, D. W.; Wang, H.-L.; Helgeson, R.; Wudl, F.; Whitten, D. G. Highly Sensitive Biological and Chemical Sensors Based on Reversible Fluorescence Quenching in a Conjugated Polymer. *Proc. Natl. Acad. Sci. U.S.A.* **1999**, *96*, 12287–12292.
14. Fan, R.; Vermesh, O.; Srivastava, A.; Yen, B. K. H.; Qin, L.; Ahmad, H.; Kwong, G. A.; Liu, C. C.; Gould, J.; Hood, L.; *et al.* Integrated Barcode Chips for Rapid, Multiplexed Analysis of Proteins in Microliter Quantities of Blood. *Nat. Nanotechnol.* **2008**, *26*, 1373–1378.
15. Kim, S. K.; Lee, S. B. Highly Encoded One-Dimensional Nanostructures for Rapid Sensing. *J. Mater. Chem.* **2009**, *19*, 1381–1389.
16. Andrew, P.; Barnes, W. L. Energy Transfer across a Metal Film Mediated by Surface Plasmon Polaritons. *Science* **2004**, *306*, 1002–1005.
17. Barnes, W. L.; Dereux, A.; Ebbesen, T. W. Surface Plasmon Subwavelength Optics. *Nature* **2003**, *424*, 824–830.
18. Hu, M.; Chen, J.; Li, Z. Y.; Au, L.; Hartland, G. V.; Li, X.; Marquez, M.; Xia, Y. Gold Nanostructures: Engineering Their Plasmonic Properties for Biomedical Applications. *Chem. Soc. Rev.* **2006**, *35*, 1084–1094.
19. Park, D. H.; Kim, M. S.; Joo, J. Hybrid Nanostructures Using π-Conjugated Polymers and Nanoscale Metals: Synthesis, Characteristics, and Optoelectronic Applications. *Chem. Soc. Rev.* **2010**, *39*, 2439–2452.
20. Park, D. H.; Kim, M.; Kim, M. S.; Kim, D. C.; Song, H.; Kim, J.; Joo, J. Electrochemical Synthesis and Nanoscale Photoluminescence of Poly(3-butylthiophene) Nanowire. *Electrochem. Solid-State Lett.* **2008**, *11*, K69–K72.
21. Garreau, S.; Louarn, G.; Buisson, J. P.; Froyer, G.; Lefrant, S. *In Situ* Spectroelectrochemical Raman Studies of Poly(3,4-ethylenedioxythiophene) (PEDT). *Macromolecules* **1999**, *32*, 6807–6812.
22. Park, D. H.; Kim, H. S.; Lee, Y. B.; Ko, J. M.; Lee, J. Y.; Kim, H. J.; Kim, D.-C.; Kim, J.; Joo, J. Light Emission of a Single Strand of Poly(3,4-ethylenedioxythiophene) (PEDOT) Nanowire. *Synth. Met.* **2008**, *158*, 90–94.
23. Joo, J.; Park, D. H.; Jeong, M.-Y.; Lee, Y. B.; Kim, H. S.; Choi, W. J.; Park, Q.-H.; Kim, H.-J.; Kim, D.-C.; Kim, J. Bright Light Emission of a Single Polythiophene Nanotube Strand with a Nanometer-Scale Metal Coating. *Adv. Mater.* **2007**, *19*, 2824–2829.
24. Park, D. H.; Kim, M. S.; Cho, E. H.; Park, S. H.; Song, H.; Kim, D. C.; Kim, J.; Joo, J. Luminescent Efficiency and Color for Poly(3-butylthiophene) Nanowires through Metal Coating: Color CCD Confirmation. *Electrochem. Solid-State Lett.* **2009**, *12*, K5–K9.
25. Liu, G. L.; Yin, Y.; Kunchakarra, S.; Mukherjee, B.; Gerion, D.; Jett, S. D.; Bear, D. G.; Gray, J. W.; Alivisatos, A. P.; Lee, L. P.; *et al.* A Nanoplasmonic Molecular Ruler for Measuring Nuclease Activity and DNA Footprinting. *Nat. Nanotechnol.* **2006**, *1*, 47–52.
26. Nam, J.-M.; Thaxton, C. S.; Mirkin, C. A. Nanoparticle-Based Bio-Bar Codes for the Ultrasensitive Detection of Proteins. *Science* **2003**, *301*, 1884–1186.
27. Han, M.; Gao, X.; Su, J. Z.; Nie, S. Quantum-Dot-Tagged Microbeads for Multiplexed Optical Coding of Biomolecules. *Nat. Biotechnol.* **2001**, *19*, 631–635.
28. Park, D. H.; Kim, B. H.; Jang, M. G.; Bae, K. Y.; Joo, J. Characteristics and Photoluminescence of Nanotubes and Nanowires of Poly(3-methylthiophene). *Appl. Phys. Lett.* **2005**, *86*, 113116-1–113116-3.
29. Lee, S. H.; Park, D. H.; Kim, K.; Joo, J.; Kim, D. C.; Kim, H. J.; Kim, J. Confocal Microscope Photoluminescence and Electrical Characteristics of Single Poly(3-hexylthiophene) Nanowire Strand. *Appl. Phys. Lett.* **2007**, *91*, 263102-1–263102-3.
30. Park, D. H.; Lee, Y. B.; Cho, M. Y.; Kim, B. H.; Lee, S. H.; Hong, Y. K.; Joo, J. Fabrication and Magnetic Characteristics of Hybrid Double Walled Nanotube of Ferromagnetic Nickel Encapsulated Conducting Polypyrrole. *Appl. Phys. Lett.* **2007**, *90*, 93122-1–93122-3.
31. Hong, Y. K.; Park, D. H.; Park, S. K.; Song, H.; Kim, D.-C.; Kim, J.; Han, Y. H.; Park, O. K.; Lee, B. C.; Joo, J. Tuning and Enhancing Photoluminescence of Light-Emitting Polymer Nanotubes through Electron-Beam Irradiation. *Adv. Funct. Mater.* **2009**, *19*, 567–572.
32. Kim, H. J.; Kim, D.-C.; Kim, R.; Kim, J.; Park, D. H.; Kim, H. S.; Joo, J.; Suh, Y. D. Confocal Raman Spectroscopy of Single Poly(3-methylthiophene) Nanotubes. *J. Appl. Phys.* **2007**, *101*, 053514-1–053514-4.